Structural Insights into Shrimp Nodavirus Capsids: New Capsid Structures to Understand the Mechanisms of Capsid Assembly and Infection

From a combination of X-ray crystal and cryo-EM structural data, the shrimp nodavirus capsid structures at atomic resolution provide structural information about mechanisms for viral assembly and infection, and be applicable to the development of an antiviral vaccine.

In many countries aquaculture is a major global economic activity, such as for the cultivation of marine fish and prawn. Taiwan, an island surrounded by sea, is a major distant-water fishery and aquaculture producer in the world.[1] *Macrobrachium rosenbergii* (*M. rosenbergii*) and *Penaeus vannamei*, (*P. vannamei*) commonly known as *giant freshwater prawn* and *Pacific white shrimp*, respectively, are economically important cultured prawns for 90% of the shrimp aquaculture industry. Notably, one major factor that limits the expansion of the shrimp culture is the constant appearance of infectious diseases caused by several viruses such as taura syndrome virus (TSV), infectious hypodermal and hematopoietic necrosis virus (IHHNV), white-spot syndrome virus (WSSV) and shrimp nodaviruses, such as *Macrobrachium rosenbergii* nodavirus (MrNV) and *Penaeus vannamei* nodavirus (PvNV), which have impacted great economic losses.[2] To date, there is no high-resolution structural information available to allow us to elucidate the capsid-related organization of the shrimp nodavirus.

Virus-like particles (VLPs), which are composed of multiple copies of one or more viral proteins, are supramolecular assemblages with well-defined geometry and have generally icosahedral or rod-like structures that mimic the overall structure of the native virions. Based on the natural intrinsic ability of structural viral subunits, these major capsid proteins (CPs) can spontaneously self-assemble into VLPs when they are expressed using recombinant expression systems from mammalian cells to bacteria. Various purposes of VLP have been widely studied and used for a drug delivery system, gene therapy, vaccine development and epitope display.[3] To investigate the properties of shrimp nodavirus capsids, a research team led by Chun-Jung Chen (NSRRC) and his co-workers solved the cryo-EM structures of $T = 3$ and $T = 1$ PvNV-like particles (PvNV-LPs) at 3.5 and 3.7 Å, respectively, crystal structures of the protrusion domains (Pds) of PvNV and MrNV in various forms at high resolution beyond 1.2 Å, and crystal structures of the $T = 1$ sub-viral particle (SVP) of the ΔN-ARM-PvNV shell domain (Sd) at resolution 3.1 Å. All diffraction data sets were collected at **TPS 05A**, **TLS 13C1** and **TLS 15A1** and **SP 44XU**.[4]

As shown in **Fig. 1(a)**, visualization with a cryo-EM showed that these capsids exist in multiple conformations, including mostly virion-sized $T = 3$ particles of diameter ~35 nm and a minor proportion of smaller-sized $T = 1$ particles ~24 nm. The resolutions of the $T = 3$ and $T = 1$ PvNV-LPs were estimated to be 3.5 and 3.7 Å according to the gold-standard Fourier shell correlation (FSC) = 0.143 criterion, respectively, after applying a soft spherical mask on the two reconstructions refined from half of the data sets independently (**Fig. 1(b)**). The cryo-EM maps clearly show $T = 3$ and $T = 1$ icosahedral symmetries composed of 180 copies and 60 copies with CP of full length 37-kDa in total, respectively (**Fig. 1(c)**). In total 90 spikes of $T = 3$ PvNV-LP are distributed along the icosahedral two-fold axes and the quasi-two-fold axes on the surface. The icosahedral asymmetric unit (iASU) within the $T = 3$ PvNV-LP contains three CPs occupying inequivalent sites with somewhat varied conformations, which are henceforth referred to as A-C subunits. The cryo-EM map allowed modeling of residues 64–368 for subunits A and B, and residues 31–368 for subunit C (**Fig. 1(d)**). Interestingly, in the $T = 3$ PvNV-LP, the ordered linkers from the subunit C/C dimer exhibit a parallel structure at the opposite side, whereas the linkers from the subunit A/B dimer adopt another new structural feature with a cross conformation (**Fig. 1(e)**).

The $T = 3$ and $T = 1$ PvNV-LPs have obviously similar structures of the S-domain, linker and P-domain, but the N-ARM and N-arm of $T = 1$ PvNV-LP are more flexible. In contrast with the $T = 3$ PvNV-LP, $T = 1$ PvNV-LP, with only A/A dimers, has a bent conformation and a smaller inner cavity and would associate weakly with the RNA nucleotide, rendering free or partial viral genome encapsidation. As mentioned above, however, the authors postulated that the association between a C/C dimer and a nucleotide might be implicated

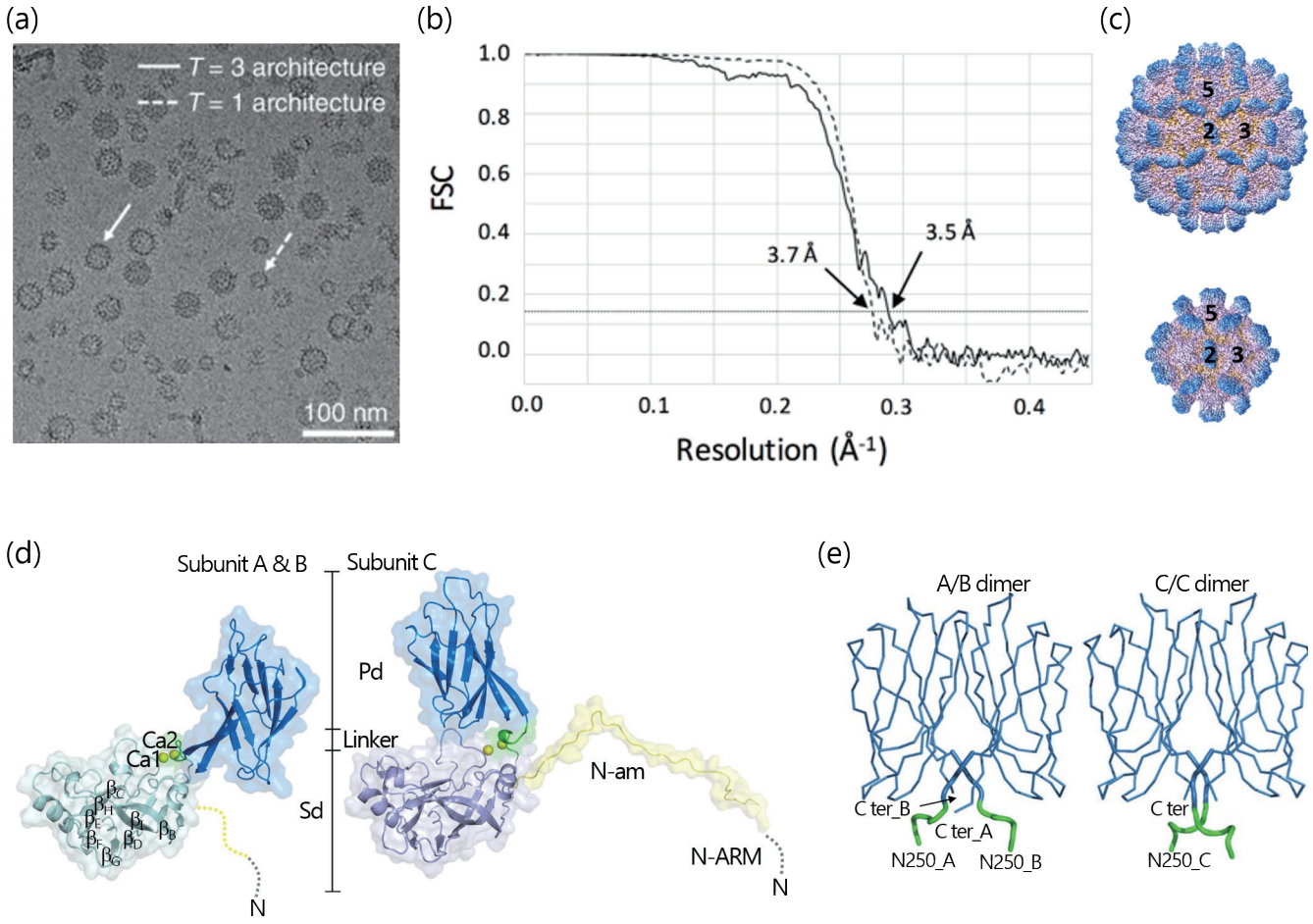

Fig. 1: (a) Cryo-EM image of PvNV-LP. The diameters of the PvNV-LPs are near 35 and 24 nm, corresponding to the $T=3$ and $T=1$ particles. $T=3$ and $T=1$ capsids are indicated with white solid and dotted arrows, respectively. Scale bar = 100 nm. (b) Fourier shell correlation (FSC) curves of the 3D reconstructions of $T=1$ (*dashed line*) and $T=3$ (*solid line*) PvNV-LPs. (c) Front view of the cryo-EM maps along an I2-symmetry axis with two-, three- and five-fold axes as indicated. The capsid surfaces are five-colored according to their distances from the particle center (red: short distance; blue: long distance). (d) Ribbon diagrams and molecular surfaces of subunits A and B, and C with bound Ca^{2+} ions (yellow spheres), comprising several domains and regions, including N-ARM (N-terminal arginine-rich motif; grey), N-arm (N-terminal arm; yellow), S-domain (light green and purple), linker (green) and P-domain (blue), respectively. (e) The homo-dimeric P-domains and linkers from the A/B and C/C dimers are color-coded as in (c) Asn250 and the *C*-termini are indicated. [Reproduced from Ref. 4]

in a size switch between $T=1$ and $T=3$ particles, and proposed a mechanistic model framed around a nucleotide-mediated C/C dimer and the A/B ($T=3$ capsid) or A/A dimer ($T=1$ capsid) with parallel and cross conformations of linkers, respectively, to explain the dynamic assemblies of the $T=1$ and $T=3$ PvNV-LPs.

Consistent with the cryo-EM structure, the crystal structures PvNVPd and MrNVPd form a dimeric straight rod with dimensions length ~40 Å and width ~22 Å in crystal packing (**Figs. 2(a) and 2(b)**). The secondary-structural elements are shown in **Figs. 2(c) and 2(d)**. The structural folds of PvNVPd and MrNVPd consist of eight β-strands, differing from that of any other known viral CP. The P-domain monomer folds into the core jelly-roll topology, forming a β-sandwich face-to-face with two pairs of antiparallel β-sheet. Four highly exposed turn insertions β1/β2, β3/β4, β5/β6 and β7/β8 appear on the top regions of PvNVPd and MrNVPd and might play an important role in the determination of the antigenicity. In the dimeric structures of PvNVPd and MrNVPd, the domain-domain contacts at the interface are two-fold symmetrically formed with a hydrogen-bond network between the main chains of the antiparallel β-strands, β3 and β6 (**Figs. 2(c)–2(e)**). Several residues are involved in these interactions, including Ala293-Gln297 and Val327-Ser331 for PvNVPd and Tyr293-Arg296 and Ile326-Asp329 for MrNVPd (**Figs. 2(d)–2(f)**). In addition, the MrNVPd dimer is stabilized with hydrogen bonds between Leu255 and Tyr257 of the β1 strand and Lys287 and Ile289 of the β3 strand (**Fig. 2(g)**).

The oligomerization of CPs is the first intermediate step during assembly of a viral capsid. As mentioned above, all structures of $T=3$ PvNV-LP, $T=1$ PvNV-LP, PvNVPd and MrNVPd at present indicate a proposed model in which the functional P-domain might be

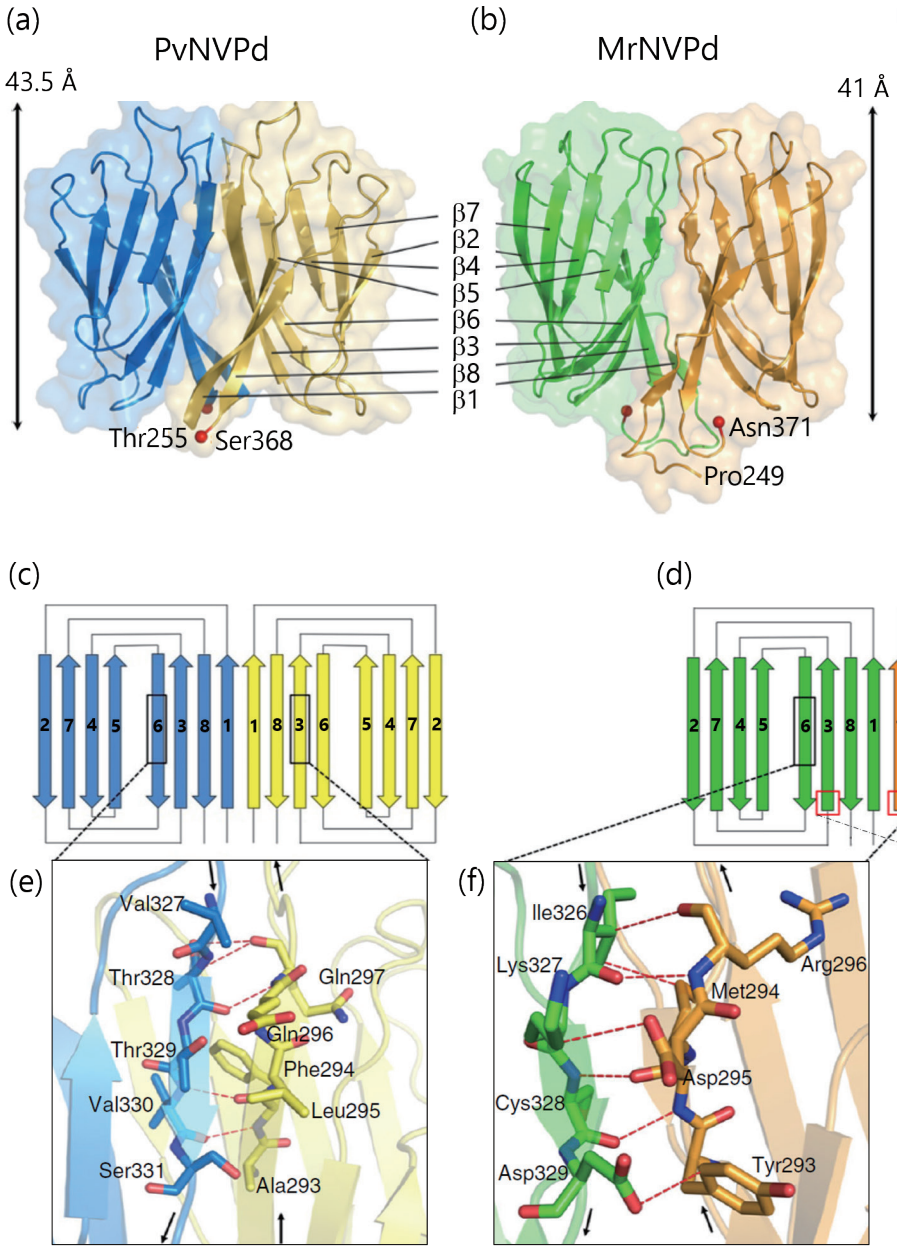

Fig. 2: (a)–(b) Ribbon diagrams and surface presentations of PvNVPd and MrNVPd are shown in similar orientations. Two C-termini are shown as red spheres. Each monomer of PvNVPd and MrNVPd is indicated in blue, yellow, green and orange, respectively. (c)–(d) Schematic diagrams of the secondary structures in PvNVPd and MrNVPd, respectively. Each monomer of PvNVPd and MrNVPd is indicated with colors as in (a) and (b). (e)–(g) The hydrogen bonds, which stabilize the dimer, from specific β-strands β1, β3 and β6 with the key residues (sticks) at the interface are shown in red. [Reproduced from Ref. 4]

involved in the dimeric capsomere formation during a capsid assembly of the shrimp nodavirus (**Fig. 3**). The N-ARM has previously been shown to play a role in controlling the particle polymorphism, such as cowpea chlorotic mottle virus, SeMV, TBSV and GNNV.[5] The crystal structure of the truncated PvNVSd (ΔN-ARM-PvNVSd) was eventually determined at resolution 3.1 Å to reveal a $T=1$ SVP architecture (**Fig. 3**). To clarify whether fusion segments on recombinant PvNV CPs affect the assembly of these multiple conformational particles, the authors found that the pET21-PvNV-LP containing the N/C-termini fusion segments might have the propensity to self-assemble into highly irregular particles of the $T=1$ architecture (**Fig. 3**).

In summary, five conclusions have been drawn according to the structural information and biochemical data. (1) The homodimeric capsomeres formed by a single CP could assemble into the complete $T=3$ virus shells, differing significantly from the other two major genuses of family *Nodaviridae*. (2) The linker exhibits cross and parallel structural forms in the $T=3$ PvNV-LP, which have not previously been recognized in any other viral CP structures. (3) The functional dimeric PvNVPd and MrNVPd exhibit a new jelly-roll structure to form cuboid-like spikes for CP dimerization through intermolecular hydrogen bonds in the initial capsid assembly. (4) The crystal structures of PvNVPd and MrNVPd, together with the cryo-EM structures of $T=3$ PvNV-LP and MrNV-LP, reveal new surface structures and morphologies of the shrimp nodaviruses as a consequence of the semi-flexibility of their linkers. (5) The N-ARM, the inherent flexibility of the N/C-terminus of PvNV CP and nucleotide encapsidation serve as a molecular switch to lead to the spontaneous

self-assembly of the PvNV capsid, resulting in particle polymorphism for $T=3$ or $T=1$ assemblies.

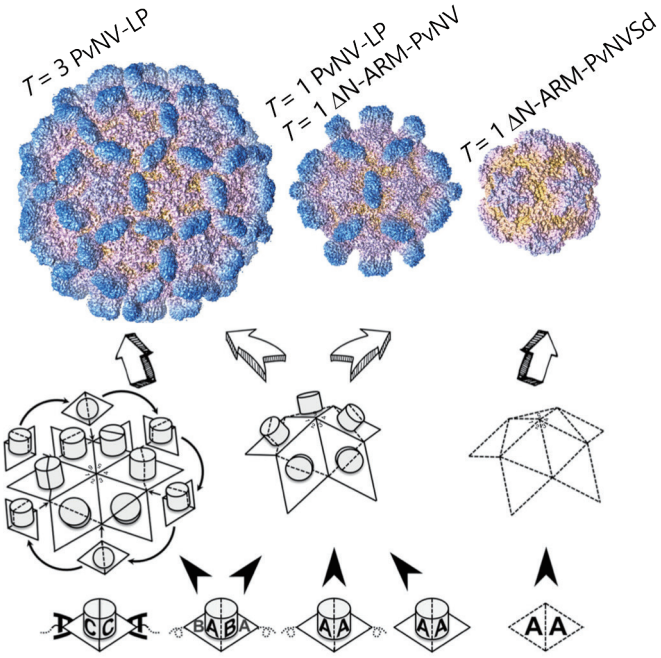

Fig. 3: Particle polymorphism and self-assembly mechanisms of shrimp nodavirus. Cryo-EM, X-ray crystal and EM structures of the $T=3$ and $T=1$ PvNV-LPs, $T=1$ ΔN-ARM-PvNV SVP and $T=1$ ΔN-ARM-PvNVSd SVP. The $T=3$ PvNV-LP surface and two $T=1$ SVP surfaces are rainbow-colored according to their distance from the spike to the shell. The diagram shows the putative self-assembly of the $T=3$ and $T=1$ shrimp nodavirus capsids. The basic unit of the capsid assembly is the dimeric capsomeres (diamond with black solid and dotted lines). The N-ARM deletion and the *N*-terminal fusion tag both might guide the assembly of the $T=1$ capsid. [Reproduced from Ref. 4]

The obtained detailed crystal and cryo-EM structures of shrimp nodavirus capsids and their specific domains can provide an improved understanding of its capsid conformation and the mechanisms of the capsid assembly and viral infection, and can also be filed to provide new insight to develop an appropriate treatment with therapeutic vaccines to prevent shrimp nodavirus infection of shrimp in the shrimp-farming industry. (Reported by Nai-Chi Chen)

This report features the work of Chun-Jung Chen and his collaborators published in Commun. Biol. ***2****, 72 (2019).*

TPS 05A Protein Microcrystallography
TLS 13C1 SW60 – Protein Crystallography
TLS 15A1 Biopharmaceuticals Protein Crystallography

- Protein Crystallography
- Biological Macromolecules, Virus Structures, Life Science

References

1. C.-L. Chen, G.-H. Qiu, Mar. Policy **48**, 152 (2014).
2. P. J. Walker, J. R. Winton, Vet. Res. **41**, 51 (2010).
3. C. Y. Yong, S. K. Yeap, Z. H. Goh, K. L. Ho, A. R. Omar, W. S. Tan, Appl. Environ. Microbiol. **81**, 882 (2015).
4. N.-C. Chen, M. Yoshimura, N. Miyazaki, H.-H. Guan, P. Chuankhayan, C.-C. Lin, S.-K. Chen, P.-J. Lin, Y.-C. Huang, K. Iwasaki, A. Nakagawa, S. I. Chan, C.-J. Chen, Commun. Biol. **2**, 72 (2019).
5. N.-C. Chen, M. Yoshimura, H.-H. Guan, T.-Y. Wang, Y. Misumi, C.-C. Lin, P. Chuankhayan, A. Nakagawa, S. I. Chan, T. Tsukihara, T.-Y. Chen, C.-J. Chen, PLoS Pathog. **11**, e1005203 (2015).

Deinococcus Radiodurans Poly ADP-Ribose Glycohydrolase Structure: Exploring Bacterial Poly ADP-Ribosylation

Unlike in eukaryotes, poly ADP-ribosylation (PARylation) remains elusive in prokaryotic organisms. A combination of structural and biochemical analyses of poly ADP-ribose glycohydrolase from Deinococcus radiodurans (DrPARG) shows that DrPARG represents a previously unidentified bacterial-type PARG that equips endo-glycohydrolase activity and further deciphers the existence of PARylation in bacteria.

Poly-ADP-ribosylation (PARylation) is a ubiquitous post-translational modification involved in various cellular processes. In eukaryotes, PARylation has been widely studied for its relation to DNA damage. In cells, the production of PAR polymers is regulated mainly by the activity of abundant nuclear PARP1. Despite the abundance of PARP1, most PAR generated by DNA damage is rapidly degraded by poly ADP-ribose glycohydrolase (PARG).